American Mineralogist, Volume 79, pages 1153–1158, 1994

Rapid-quench hydrothermal experiments at mantle pressures and temperatures

Craig E. Manning, Scott L. Boettcher
Department of Earth and Space Sciences, University of California, Los Angeles, Los Angeles, California 90024-1567, U.S.A.

Abstract

New experimental methods for the encapsulation, extraction, and analysis of large volumes of aqueous fluids enable studies of mineral solubilities and dissolution kinetics with the piston-cylinder apparatus. Quench rates and volumes of experimental fluids with these methods are comparable with those used in modern hydrothermal experiments employing cold-seal vessels. Analyses of fluid compositions are reproducible and consistent with independent results. The techniques permit experimental investigations that will better characterize fluid-rock interaction in such environments as subducting slabs, the mantle wedge, Barrovian metamorphic belts, and middle to lower crustal granulites.

Introduction

Elemental mass transport by aqueous fluids plays a central role in petrologic processes in many medium- and high-pressure environments. For example, metasomatism of the mantle wedge by aqueous fluids from subducting slabs (e.g., Fyfe and McBirney, 1975; Wyllie, 1979) may govern the origin and composition of arc magmas. In addition, mineral dissolution and elemental transport can dramatically alter bulk compositions in Barrovian metamorphic belts (e.g., Ague, 1991).

Quantitative studies of metasomatic mass transfer require experimental measurements of the solubilities and dissolution rates of minerals in aqueous fluids. The accuracy and precision of such measurements depends on rapid quench rates and, for complex mineral-fluid systems, the controlled extraction and analysis of experimental fluids (Eugster et al., 1987). Although a variety of robust methods now exist for hydrothermal experiments below about 4 kbar (e.g., Ulmer and Barnes, 1987; Holloway and Wood, 1988), experimental difficulties have limited similar progress at higher pressures. The most complete data on mineral solubility above 4 kbar employed an internally heated gas apparatus (e.g., Anderson and Burnham, 1965, 1967, 1983). These results have provided the best available constraints on high-pressure solubilities of, for example, quartz and feldspar. However, the data are limited to <10 kbar and may suffer from the slow quench rates of the apparatus, which leads to precipitation of solutes from the experimental solution (Manning, 1994).

The rapid quench rates necessary for hydrothermal experiments are easily attained with the piston-cylinder apparatus, but the comparatively small volumes of experimental charges have limited its use for this purpose. Early piston-cylinder results on high-pressure mineral solubilities (e.g., Nakamura, 1974; Ryabchikov and Boettcher, 1980; Ryabchikov et al., 1982; Ryabchikov and MacKenzie, 1985; Schneider and Eggler, 1986) relied on either imprecise mass-balance techniques or drying the solution and collecting the resulting solids, both of which may have introduced large uncertainties in the solubilities inferred. Sneeringer and Watson (1985), Cemič et al. (1990), and Ayers et al. (1992) described new methods for encapsulating large fluid volumes that were successfully applied in studies of the behavior of minor and trace elements during mineral-fluid interactions at ≥ 1000 °C and >10 kbar (Ayers and Watson, 1991, 1993a; Brenan and Watson, 1991; Brenan, 1993). Similar methods have been employed to determine corundum, rutile, and quartz solubilities in H_2O (Becker et al., 1983; Ayers and Watson, 1993b; Manning, 1994). Establishing solubilities by measuring the weight lost from crystals or by changes in the composition of mineral grains, these studies demonstrated that experimental investigations of mineral solubility are now possible at high pressures for simple systems. However, expanding these investigations to more complex mineral-fluid systems requires the accurate and precise analysis of fluid compositions. Here we describe techniques that enable such analyses for experimental solutions generated at high pressures using a piston-cylinder apparatus.

Methods

Encapsulation

A modified double-capsule method is used (Fig. 1). Individual crystals or a mixture of crushed grains are placed in an inner Au capsule with a 2-mm o.d. The capsule is not welded but rather crimped and folded shut to allow fluid from the outer capsule to equilibrate with the solid starting materials. The inner capsule is not required for the measurement of solubility, but it prevents large single crystals from breaking or crushing if they wedge into a corner of the outer capsule. The Au capsule, additional compounds such as NaCl or oxides, and 50–75 μL of H_2O are loaded into a Pt capsule with a 5-mm o.d. and a triple-crimped and welded base. The outer Pt capsule

0003–004X/94/1112–1153$02.00

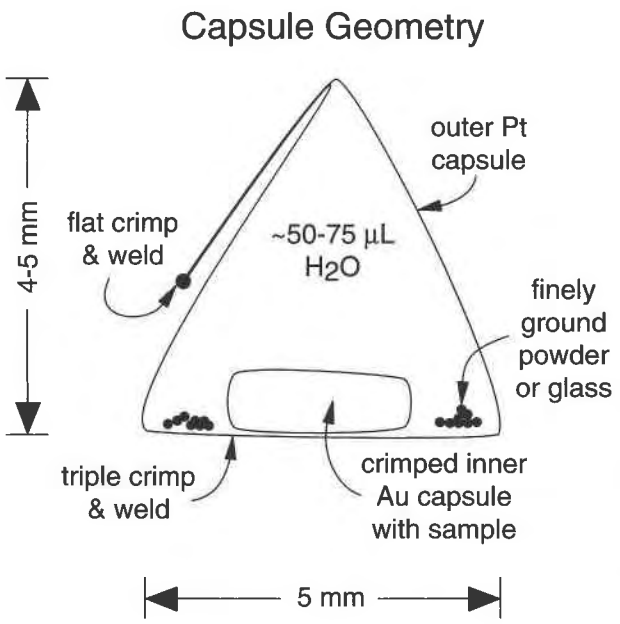

Fig. 1. Schematic illustration of the capsule shape and dimensions.

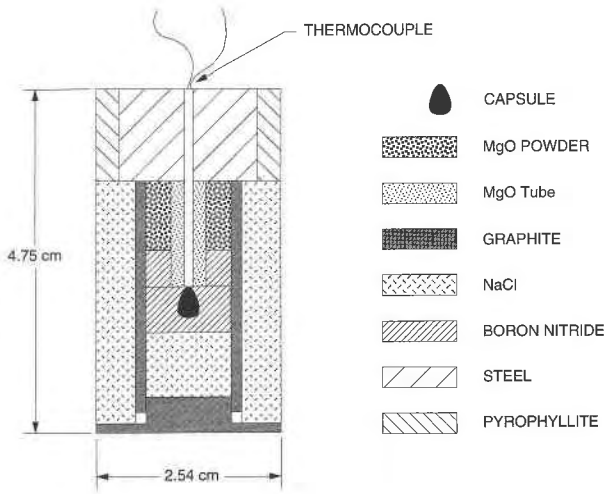

Fig. 2. NaCl + graphite furnace assembly for hydrothermal experiments.

is then crimped flat, weighed, sealed by arc welding, and then weighed again. The multiple weighings identify H_2O loss during each step. Fluid volumes of 50–75 μL compare favorably with the 80–100 μL of hydrothermal experiments in rapid-quench cold-seal experiments (e.g., Eugster et al., 1987). The final capsule height is typically 4–5 mm. The flat-crimped top and triple-crimped base are strong points in the capsule, whereas the sloping walls expand or contract to accommodate volume changes of the solvent (Fig. 1). Alternative methods of encapsulation, some of which avoid the difficult welding step, may also be used to fit the experimental task at hand (Sneeringer and Watson, 1985; Cemič et al., 1990; Ayers et al., 1992).

Furnace assembly

The furnace assembly is 2.54 cm in diameter and made primarily of NaCl and graphite (Fig. 2), following the design of Bohlen (1984). The capsule is oriented vertically in the furnace such that its center corresponds to the furnace midpoint, or hot spot, where temperature is greatest. Powdered boron nitride (BN) is packed around the capsule, and a BN ring is placed above it. In addition to decreasing temperature gradients, this minimizes the NaCl adhering to the capsule after the experiment, which is important if the fluid is to be analyzed for Na or Cl. The outer NaCl cylinder is pressed to a length 1.8 mm longer than the graphite heater, leaving a gap to accommodate furnace compression due to compaction of the powdered BN (Fig. 2).

Temperatures are measured with Pt-$Pt_{90}Rh_{10}$ thermocouples sheathed in mullite and MgO tubes and resting on a piece of Pt foil on the folded top of the capsule. The large furnace diameter leads to the potential for sharp drops in temperature near the hot spot. Temperature gradients are decreased by using thick, 3.4-mm graphite heaters to generate a broader hot spot. Figure 3 shows the variation of the temperature difference between the hot spot and a point 4 mm above the hot spot ($\Delta T = T_{+4\text{ mm}} - T_{\text{hot spot}}$) with the thick graphite heater. Measurements were made with no capsule in the furnace using two thermocouples simultaneously. There was no temperature difference below 500 °C at 10 kbar. Above 500 °C, ΔT decreased to −13 °C at 1000 °C (Fig. 3). Linear regression of temperature differences measured at intervals of 50 °C gave $\Delta T = 12.27 - 0.025T$. Thus, in an 8-mm capsule centered on the hot spot, the maximum temperature difference between the capsule's center and its ends would be ~13 °C at a temperature of 1000 °C. Because the capsules described above are 4–5 mm long, the maximum temperature difference at the same nominal temperature can be assumed to be 7 °C. However, it is likely that the gradients are smaller still, since temperature gradients are not linear (e.g., Ayers et al., 1992), and the presence of a capsule decreases the temperature gradient in the furnace. It is important to note that the more massive graphite heater generates significantly more heat at a given temperature during experiments, which may cause cooling problems if experimental temperatures are high. Moreover, should this furnace design be used for experiments above ~1100 °C, it may require increasing the kilovolt-amp rating of the transformer.

Piston-cylinder methods and calibration

The hydrothermal experiments employ a piston-in technique in which first pressure and then temperature are increased in steps until the desired conditions are attained. Pressure and temperature are stepped up succes-

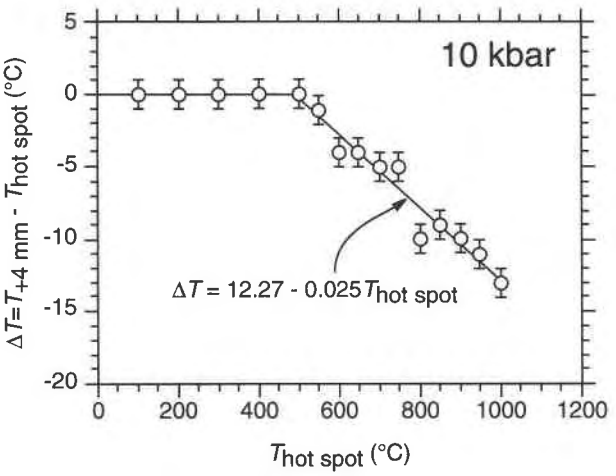

Fig. 3. Temperature gradients in furnace assembly; ΔT is the difference between the hot-spot temperature and that 4 mm above the hot spot. The line was fitted by linear least squares.

sively to ensure that the volume of H_2O is within ~10% of the final experimental value. By preventing large variations in fluid volume, the capsule is less likely to fail.

The use of a piston-cylinder apparatus for hydrothermal experiments enables rapid quench rates because thermal energy is concentrated in a small volume. Thus, by simply cutting power to the system, experiments can be quenched to <50 °C in <~1 min. An example of the utility of these advantageous quench rates was discussed by Manning (1994) using experiments on the solubility of quartz in H_2O. This study showed that using the same encapsulation and measurement methods, discrepancies between solubilities measured in a piston cylinder and those obtained with an internally heated gas apparatus (Anderson and Burnham, 1965) were explained by variations in quench rate.

Because many of the solubility experiments for which our assembly is used focus on relatively low temperatures and high pressures, the albite + jadeite + quartz equilibrium at 600 °C was used to ensure that the entire assembly had low strength. The equilibrium was located between 16.6 and 17.0 kbar (Table 1). This agrees well with previous results of 16.5 ± 0.5 (Hays and Bell, 1973) and 16.4 ± 0.4 kbar (Bohlen, 1984) and is several hundred bars above the reversal of 16.25 ± 0.25 kbar of Holland (1980), indicating that the friction correction for this assembly is negligible.

Fluid extraction

Eugster et al. (1987) outlined a routine for puncturing capsules and extracting fluids in a glove box. Our concerns about our somewhat smaller solution volumes, the risk of spattering of solution on capsule puncturing, and our ability to completely withdraw fluids before incipient evaporation led to the construction of the two-piece extraction vessel shown in Figure 4. Both the base and the top of this vessel were machined from Teflon and threaded so that the top can be driven downward with a screwing action. The top was fitted with O rings to ensure a tight seal. Small, aligned openings in the top and bottom pieces of the vessel allow air to escape. This device can be used in a glove box with an Ar atmosphere if contamination by O_2 or CO_2 is a concern.

Table 1. Results of furnace calibration experiments using the equilibrium albite = jadeite + quartz

Expt.	T (°C)	P (kbar)	t (h)	Result	Comments
198	600	16.6	48	ab	slight ab growth
199	600	16.6	52	ab	slight ab growth
200	600	17.4	49	jd + qz	strong jd + qz growth
201	600	17.0	49	jd + qz	
219	600	16.6	42.5	ab	

After removal from the furnace assembly, the capsule was rinsed for several minutes in dilute HF and distilled H_2O to clean the outer surface of adhering BN. The capsule was placed in the well in the base of the extraction vessel with a diluting solution. The composition and volume of this solution can be varied, depending on the nature of the experiment and fluid concentration; we generally acidify with 15 mL of 5% HNO_3 to ensure that dissolved solids in these concentrated fluids remain in solution. Controls should be used to establish that the diluting solution does not dissolve experiment products. For example, we observed no measurable solubility of single crystals of quartz, kyanite, and corundum in 5% HNO_3 after 1 week at 25 °C and 1 atm.

To puncture the capsule, the vessel top is screwed downward so that the protruding steel pointer pierces the submerged capsule. Because the capsule is submerged, no loss of experimental fluid occurs. The top is withdrawn slightly, and the vessel is gently tapped to separate the capsule from the steel tip. After fully mixing, the resulting solution is decanted and analyzed by the desired technique. The physical state of the quench solutions varies greatly, depending on the concentrations of dissolved sol-

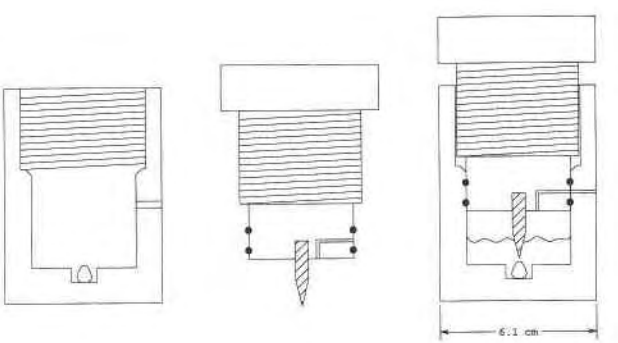

Fig. 4. Vessel for extracting solutions from hydrothermal experiments. High-angle ruling denotes stainless steel and low-angle ruling denotes threading; unruled regions areTeflon.

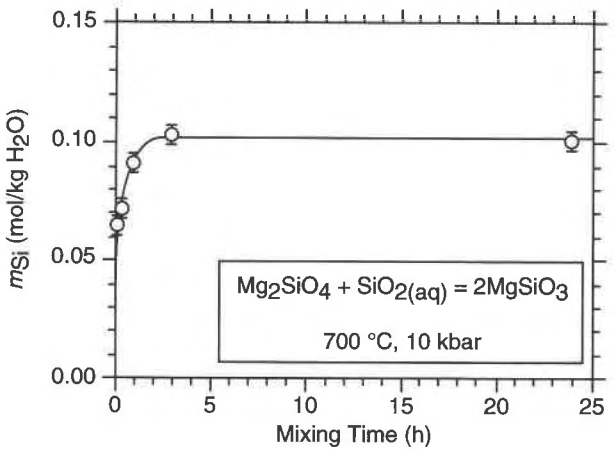

Fig. 5. Variation in the apparent solubility with the time of fluid mixing in an extraction vessel. Uncertainties are 2 sd (±0.008 mol/kg H_2O).

ids. At low to moderate concentrations, the quench solution may precipitate no material or it may be a colloidal suspension. In the case of colloidal suspensions, the acidifying solution should be selected so that it redissolves the particulate material to allow accurate determination of fluid composition at the pressure and temperature of the experiment. However, if concentrations of dissolved solids or mineral growth rates are too great, the growth of new crystals or overgrowths may prevent accurate use of the techniques described here.

The time required to mix fully the fluids prior to analysis was evaluated using the reaction

$$\underset{\text{forsterite}}{Mg_2SiO_4} + SiO_{2(aq)} = \underset{\text{enstatite}}{2MgSiO_3}.$$

Experiments were conducted at 700 °C and 10 kbar for 24 h using crystals 2–3 mm in size of Bamble enstatite (X_{Mg} = 0.86) and San Carlos forsterite (X_{Mg} = 0.90). Procedures outlined above were followed for five experiments, varying only the time that each capsule was left in 5% HNO_3 solution after puncturing (Table 2). No quench solids remained in the capsule after fluid extraction, and scanning electron microscopy revealed no quench iron or magnesium oxides on the surfaces of pyroxene or olivine grains. Fluids were analyzed for Si, Mg, and Fe concentrations by ICP. Both Mg and Fe were below detection at this level of dilution, indicating concentrations of <200 ppm in the experimental fluids. Figure 5 illustrates the change in Si concentration, with time allowed for fluid mixing after puncturing, showing that at least 2 h are required for full extraction and homogenization in the absence of any agitation. In practice, this time can probably be decreased by periodic swirling or by plugging the air hole and advancing and withdrawing the top in a pumping action. However, care must be taken to avoid disaggregating the grains where delicate textures must be preserved.

Table 2. Experimental results testing the extraction vessel

Expt.	T (°C)	P (kbar)	t (h)	Mixing t (h)	Si* (m)	Si** (m)
			$Mg_2SiO_4 + SiO_{2(aq)} = 2MgSiO_3$			
390	700	10	24	0.33	—	0.071
391	700	10	24	0.08	—	0.064
393	700	10	24	1.0	—	0.091
394	700	10	24	3.0	—	0.103
392	700	10	24	24.0	—	0.100
			$SiO_{2(quartz)} = SiO_{2(aq)}$			
430	500	12.5	67	3.0	0.180	0.184
431	600	5	92	3.0	0.216	0.224
432	600	5	89	3.0	0.228	0.216

* Si concentration by weight loss; 1 sd = 0.020 m (Manning, 1994).
** Si concentration by ICP analysis; 1 sd = 0.004 m, derived by pooling the results of two to three replicate ICP analyses per experiment.

Experiments on quartz solubility in H_2O were used to assess the accuracy of the fluid extraction method. Because quartz dissolves congruently, the weight loss from single crystals provides an independent solubility determination for comparison with results from the techniques described above. Table 2 gives the results from three experiments on quartz solubility in H_2O. The Si concentrations measured by the two techniques agree closely. Also, the repeated experiments 431 and 432 demonstrate excellent reproducibility. The agreement between the two analytical methods shows that if silica is precipitated during quench, (1) it does not do so by growing on the single crystal, and (2) the precipitate is redissolved by the diluting solution. However, it should be recognized that mineral solubilities in aqueous solutions are generally high at the conditions for which these methods will be used, and careful experiments that check for quench problems in the particular system being investigated should always be carried out.

Applications

The new methods allow experimental investigations of fluid compositions at pressures and temperatures that have previously been inaccessible. Manning (1994) used many of these techniques to investigate quartz solubility in H_2O to 20 kbar and 900 °C. Studies of equilibrium solubilities in H_2O have been extended to more complex minerals such as kyanite, magnesium silicates (forsterite and enstatite), and sodium and aluminum silicates (jadeite and albite), all of which dissolve incongruently (e.g., Manning, 1993). Mineral solubilities involving more complex fluids containing NaCl, HCl, or CO_2 can be readily investigated using the techniques described. Moreover, because of the controlled fluid-extraction routine, the methods can be used with pH and f_{O_2} buffering to investigate speciation of metals at high pressures using methods similar to those in cold-seal pressure vessels (e.g., Eugster, 1986; Eugster et al., 1987).

Studies of the kinetics of mineral dissolution in aqueous fluids are also aided by these techniques. Such studies require not only the accurate and precise analysis of fluid compositions but also the preservation and interpretation

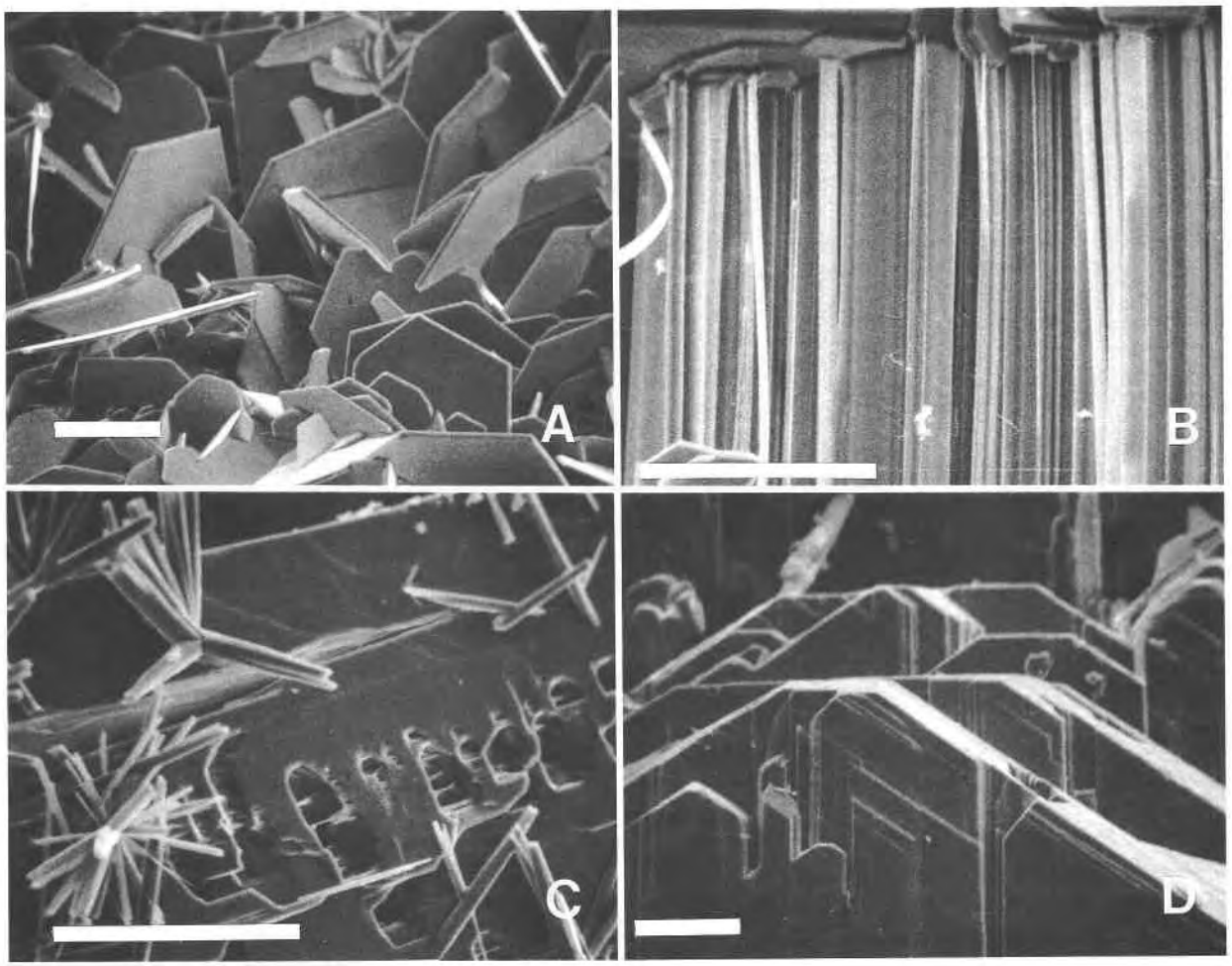

Fig. 6. Secondary electron micrographs illustrating textures of kyanite dissolution and growth. Scale bars are 15 μm. (**A**) Hexagonal corundum platelets coating kyanite surface (no. 369, 700 °C, 10 kbar, 24 h). (**B**) Linear etch grooves parallel to the **c** crystallographic axis (no. 369, 700 °C, 10 kbar). (**C**) Acicular diaspore sprays on kyanite surface. The kyanite crystal displays well-developed etch pits (no. 388, 400 °C, 10 kbar, 70 h). (**D**) Subhedral kyanite terminations grown by adding finely ground Al_2O_3 and quartz powders to supersaturate solution with respect to kyanite (no. 404, 700 °C, 10 kbar, 94 h).

of dissolution and growth textures. The large fluid volumes afford a hydrostatic environment, which preserves important textural relations. Figure 6 illustrates the range of delicate textures exhibited by experiments on the dissolution of natural kyanite grains in H_2O. Each experiment contained several cleavage flakes 4–5 mm in size from larger, gem-quality kyanite crystals (Bahia, Brazil; 0.20 wt% Fe_2O_3: Bohlen et al., 1991). In experiments in which kyanite reacted with pure H_2O at 700 °C and 10 kbar, a dense network of hexagonal corundum platelets completely coated the kyanite crystal (Fig. 6A). Disaggregating this coating revealed that the kyanite surface developed linear etch grooves on 100 and 010 crystal faces (Fig. 6B). The grooves are elongate parallel to the **c** crystallographic axis and probably formed preferentially along cleavage planes. Locally, acicular kyanite strands may separate from the main crystal (Fig. 6B). Products from similar experiments at 400 °C and 10 kbar displayed acicular sprays of diaspore on kyanite surfaces (Fig. 6C). The formation of etch pits at these lower temperatures (Fig. 6C) instead of etch grooves (Fig. 6B) implies a change in the dissolution texture of kyanite with temperature.

Finally, hydrothermal growth processes and textures of high-pressure phases can also be explored. Figure 6D illustrates growth textures formed on a kyanite surface at 700 °C and 10 kbar. The fluid was supersaturated by loading finely ground powders of Al_2O_3 and quartz with H_2O and kyanite crystals. It is assumed that powders dissolve quickly relative to kyanite, forming a supersaturated solution that then precipitates kyanite on the cleavage flakes. The subhedral terminations and steps illustrated in Figure 6D are consistent with this interpretation.

Acknowledgments

This work was supported by NSF grants EAR-9104288 and EAR-9205956. S. Wong took the photomicrographs and devoted long hours to

the study of dissolved kyanite grains; S. Bohlen and A. Montana offered advice; D. Winter aided the ICP analyses; and J. Ayers, J. Brenan, K. Knesel, and H. Lin provided helpful comments that improved the manuscript.

References cited

Ague, J.J. (1991) Evidence for major mass transfer and volume strain during regional metamorphism of pelites. Geology, 19, 855–858.

Anderson, G.M., and Burnham, C.W. (1965) The solubility of quartz in supercritical water. American Journal of Science, 263, 494–511.

——— (1967) Reactions of quartz and corundum with aqueous chloride and hydroxide solutions at high temperatures and pressures. American Journal of Science, 265, 12–27.

——— (1983) Feldspar solubility and the transport of aluminum. American Journal of Science, 283-A, 283–297.

Ayers, J.C., and Watson, E.B. (1991) Solubility of apatite, monazite, zircon and rutile in supercritical aqueous fluids with implications for subduction zone geochemistry. Philosophical Transactions of the Royal Society of London, A335, 365–375.

——— (1993a) Apatite/fluid partitioning of rare-earth elements and strontium: Experimental results at 1.0 GPa and 1000 °C and application to models of fluid-rock interaction. Chemical Geology, 110, 299–314.

——— (1993b) Rutile solubility and mobility in supercritical aqueous fluids. Contributions to Mineralogy and Petrology, 114, 321–330.

Ayers, J.C., Brenan, J.M., Watson, E.B., Wark, D.A., and Minarik, W.B. (1992) A new capsule technique for hydrothermal experiments using the piston-cylinder apparatus. American Mineralogist, 77, 1080–1086.

Becker, K.H., Cemič, L., and Langer, K.E.O. (1983) Solubility of corundum in supercritical water. Geochimica et Cosmochimica Acta, 47, 1573–1578.

Bohlen, S.R. (1984) Equilibria for precise pressure calibration and a frictionless furnace assembly for the piston-cylinder apparatus. Neues Jahrbuch für Mineralogie Monatshefte, 404–412.

Bohlen, S.R., Montana, A., and Kerrick, D.M. (1991) Precise determinations of the equilibria kyanite ⇌ sillimanite and kyanite ⇌ andalusite and a revised triple point for Al_2SiO_5 polymorphs. American Mineralogist, 76, 677–680.

Brenan, J.M. (1993) Partitioning of fluorine and chlorine between apatite and aqueous fluids at high pressure and temperature: Implications for the F and Cl content of high *P-T* fluids. Earth and Planetary Science Letters, 117, 251–263.

Brenan, J.M., and Watson, E.B. (1991) Partitioning of trace elements between olivine and aqueous fluids at high *P-T* conditions: Implications for the effect of fluid composition on trace element transport. Earth and Planetary Science Letters, 107, 672–688.

Cemič, L., Geiger, C.A., Hoyer, W.W., Koch-Müller, M., and Langer, K. (1990) Piston-cylinder techniques: Pressure and temperature calibration of a pyrophyllite-based assembly by means of DTA measurements, a salt-based assembly, and a cold sealing sample encapsulation method. Neues Jahrbuch für Mineralogie Monatshefte, 49–64.

Eugster, H.P. (1986) Minerals in hot water. American Mineralogist, 71, 655–673.

Eugster, H.P., Chou, I-M., and Wilson, G.A. (1987) Mineral solubility and speciation in supercritical chloride fluids. In G.C. Ulmer and H.L. Barnes, Eds., Hydrothermal experimental techniques, p. 1–19. Wiley, New York.

Fyfe, W.S., and McBirney, A.R. (1975) Subduction and the structure of andesitic volcanic belts. American Journal of Science, 275-A, 285–297.

Hays, J.F., and Bell, P.M. (1973) Albite-jadeite-quartz equilibrium: A hydrothermal static determination (abs.). Eos, 54, 482.

Holland, T.J.B. (1980) The reaction albite = jadeite + quartz determined experimentally in the range 600–1200 °C. American Mineralogist, 65, 129–134.

Holloway, J.R., and Wood, B.J. (1988) Simulating the Earth: Experimental geochemistry, 196 p. Unwin-Hyman, Boston.

Manning, C.E. (1993) Kyanite solubility in H_2O at 700 °C and 1 GPa and Al transport during subduction zone metasomatism (abs.). Eos, 74 (16, suppl.), 321–322.

——— (1994) The solubility of quartz in H_2O in the lower crust and upper mantle. Geochimica et Cosmochimica Acta, in press.

Nakamura, Y. (1974) The system SiO_2-H_2O-H_2 at 15 kbar. Carnegie Institution of Washington Year Book, 73, 259–263.

Ryabchikov, I.D., and Boettcher, A.L. (1980) Experimental evidence at high pressure for potassic metasomatism in the mantle of the Earth. American Mineralogist, 65, 915–919.

Ryabchikov, I.D., and MacKenzie, W.S. (1985) Interaction of jadeite with water at 20–30 kbar and 650 °C. Mineralogical Magazine, 49, 601–603.

Ryabchikov, I.D., Schreyer, W., and Abraham, K. (1982) Compositions of aqueous fluids in equilibrium with pyroxenes and olivines at mantle pressures and temperatures. Contributions to Mineralogy and Petrology, 79, 80–84.

Schneider, M.E., and Eggler, D.H. (1986) Fluids in equilibrium with peridotite minerals: Implications for mantle metasomatism. Geochimica et Cosmochimica Acta, 50, 711–724.

Sneeringer, M.A., and Watson, E.B. (1985) Milk cartons and ash cans: Two unconventional welding techniques. American Mineralogist, 70, 200–201.

Ulmer, G.C., and Barnes, H.L., Eds. (1987) Hydrothermal experimental techniques, 523 p. Wiley, New York.

Wyllie, P.J. (1979) Magmas and volatile components. American Mineralogist, 64, 469–500.

Manuscript received March 2, 1994
Manuscript accepted July 8, 1994